A multimodal approach to analysis of steady state visually evoked potentials

Nikhil Vij, Wu Zuobin, Malin Björnsdotter, Justin Dauwels*
School of Electrical and Electronics Engineering
Nanyang Technological University
Singapore 30332
*jdauwels@ntu.edu.sg

François Benoît Vialatte
SIGMA lab
ESPCI ParisTech
Paris, France

***Abstract*—Steady state visually evoked potentials (SSVEPs), recorded from the central nervous system of humans using electroencephalography (EEG) in response to visual stimuli, have recently gained attention in cognitive and clinical neuroscience [1]. Here, we fuse EEG SSVEPs with recordings from functional magnetic resonance imaging data (fMRI), utilizing the millisecond temporal resolution of the former and the excellent spatial resolution of the latter. In particular, we propose a spatio-frequency EEG/fMRI fusion framework to recover the frequency content from the EEG and spatial information from the fMRI to enhance our understanding of SSVEPs. Notably, we consider fused analysis of fMRI and EEG data collected independently. We demonstrate that the proposed approach is a practical data-driven method to achieve spatio-frequency fusion of EEG and fMRI SSVEP responses.**

I. Introduction

Sensory evoked potentials (SEPs) are electrical potentials generated by the brain in response to sensory organ stimulation. Prolonged visual stimuli consisting of sinusoidally modulated monochromatic light evoke a special type of SEP called 'steady-state visually evoked potentials" (SSVEPs). SSVEPs are periodic evoked responses, with a stationary distinct spectrum showing characteristic SSVEPs peaks, stable over time [1]. They are best observed in the frequency or time-frequency domains. SSVEPs have been studied in multiple paradigms in cognitive research (primarily regarding visual attention[2], binocular rivalry[3][4] and working memory[5]–[10]) as well as in the context of clinical neuroscience [11]–[13]. The primary technique for studying SSVEP is electroencephalography (EEG; see e.g. [14]–[17]). EEG reflects electrical activity resulting from the summation over thousands of synchronously activated post-synaptic potentials in the brain, and is measured through electrodes attached to the scalp. The time-resolution of EEG is excellent, at the level of milliseconds. However, the technique suffers from poor spatial resolution (at the level of centimeters). Magnetic resonance imaging (MRI), on the other hand, offers excellent spatial resolution. MRI involves measurements of signals derived from intrinsic atomic properties of matter and enables noninvasive detailed exploration of biological tissues [18]. In particular, local blood oxygenation changes in response to neural processing measured with functional MRI (fMRI) provides an effective, albeit indirect, indication of relative levels of brain activity [19]. In contrast, fMRI suffers from poor temporal resolution, in the range of three to four seconds. Combined, therefore, EEG and fMRI provides excellent temporal and spatial resolution, and there is a growing interest in utilizing both modalities in the study of SSVEPs (see e.g. [20], [21]). However, traditional analysis approaches to EEG and fMRI differ fundamentally. Research EEG is typically treated as time-series, where response estimates are formed from averaging over numerous events [22]. In fMRI, the governing approach is anatomically locating average activity using statistical techniques based on the general linear model and extensive t-testing [23]. Following this fragmented approach, conventional multimodal studies process data independently and, subsequently, estimate inter-modality coupling using post hoc juxtaposition through statistical correlation measures. Truly integrated analysis, in contrast, makes explicit a priori assumptions about the coupling between the modalities. The superiority of such fused analysis over juxtaposition techniques was recently demonstrated in a study of the coupling between fMRI and EEG brain activity: from an information-theory point of view, the distribution of responses from the fused modalities was more informative than any single modality [24]. In this paper, we evaluate a true fusion approach to analysis of EEG and fMRI data collected during SSVEPs. To achieve this, we used joint independent component analysis (jICA), which is a blind source separation technique that derives a spatiotemporal solution with jointly estimated maximally independent sources of between-subject effects [25].

In previous applications, the jICA framework has been used for fusion of fMRI and transient event-related potentials (ERPs) in the EEG [25]–[27]. Since the SSVEP EEG response is reflected in a stationary wave rather than a transient evoked event, however, the response is better defined in the frequency than the time domain. Nevertheless, the origin of the data is essentially irrelevant for the jICA analysis [25], [28], [29]. We therefore specifically attempted to fuse the SSVEP frequency information of the EEG with the spatial information from the fMRI.

II. Methods

We first describe the SSVEP data acquisition paradigm and subjects, common to both EEG and fMRI. We then

978-1-4673-5875-0/13/$31.00

outline the fMRI and EEG data acquisition and preprocessing, respectively. Finally, we detail the joint ICA approach.

A. SSVEP Paradigm

SSVEP stimulation consisted of flickering white screens, displayed using Avotec optic fiber goggles (Silent Vision googles, visual angle 18x24°). During stimulation, subjects observed a flickering white/black light generated with a Silent Vision shutter to control high frequency refreshment rates. During fixation, subject saw a gray background, isoluminant with the stimuli. SSVEP was evoked using 21 frequencies from 1 to 100 Hz, displayed in a pseudo-randomized order. The same sequence of frequencies was presented to all subjects. The 21 frequencies were distributed in order to regularly match the harmonics of 10 Hz: [1.0; 1.25; 1.88; 2.5; 3.3; 4.17; 5.0; 6.6; 8.3; 10.0; 13.3; 16.6; 20.0; 26.6; 33.3; 40.0; 53.3; 66.6; 80.0; 90.0; 100] Hz. Each experiment consists of 7 blocks of 9 trials separated by 1 min rest. Each trial consisted of 20 sec. of rest condition followed by 15 sec. of stimulation. Three trials were recorded for each frequency (total = 63 trials per subject).The same protocol was used both for EEG and fMRI data collection.

B. Subjects

The data were collected in RIKEN Brain Science Institute, Japan. The study was performed in accordance with the Declaration of Helsinki and approved by the ethical review board of RIKEN Brain Science Institute, Japan. Three subjects participated in the study (all females, right handed, age range 20-25).

C. fMRI acquisition and processing

Magnetic resonance imaging was performed on a 1.5T scanner. T1-weighted anatomical brain scans were acquired first (voxel size 3.75/ 3.75/ 3.75 mm), lasting approximately 20 minutes. Functional T2*-weighted gradient echo (GE) echo planar imaging (EPI) sequences with 134 dynamics were used for BOLD measurements. Four additional dynamics were used to obtain steady state of tissue magnetization. Functional EPI volumes were acquired with 25 axial AC-PC aligned slices (5 mm slice thickness, gap-less, field of view 240 x 240 m, matrix = 64 x 64 voxels) covering the entire brain. The repetition time (TR) was set to 2.583 s with echo time (TE) of 25 ms. During scanning, the subjects were shown the visual stimuli described above. The fMRI data were pre-processed in Brainvoyager QX. Pre-processing steps included realignment, co-registration, segmentation, normalization and smoothing. To improve signal-to-noise-ratio, the trials were binned into four frequency bands as follows: low=[1.0, 1.25, 1.88, 2.50, 3.33, 4.17,5.0], low-mid= [6.67, 8.33, 10.0], mid=[13.3, 16.67, 20.0] and high=[26.67, 33.3, 40.0]. First, contrast images reflecting the SSVEP stimuli vs. background for each of these frequency bands were obtained by applying a general linear model (GLM) analysis [23] in each subject. These contrast images were used in the jICA analysis. Second, we entered all subjects contrast images into a second level analysis to reveal consistent group level activations.

D. EEG acquisition and processing

In a separate session, EEG data were recorded in the same subjects in a shielded room equipment by using Biosemi, Inc. (Amsterdam, The Netherlands), caps. The Biosemi cap contained 128 active electrodes positioned according to the extended 10/20 system. The recorded signal was sampled at 1024 Hz, along with bandpass filtering in the range of 5-220Hz range. The acquired data were subject to analog bandpass filtering, and high-pass filtering with cutoff frequency of 1Hz and a reference average of all channels was subtracted. Blind source separation (BSS) was then used to clean the data of artifacts from muscle and eye movements, instrumental and other noise. BSS is a method for recovering the underlying sources from linear mixtures of signals. BSS consists recovering the unknown sources. The linear and instantaneous models of BSS can be formulated as: $x = As$, where x is observed mixture, A is mixing matrix, s represents a data matrix as rows the observed signals. The algorithm for performing BSS was second-order blind identification (SOBI). SOBI minimizes the following criterion:

$$C(A, \lambda) = [\hat{Y} - I \otimes G(A)\lambda]W[\hat{Y} - I \otimes G(A)\lambda] \quad (1)$$

where, $\hat{Y}$ is the sources to be estimated, I is the identity matrix, A is the mixing matrix, λ is the diagonal of the correlation matrix of x, G is the Kathri-Rao product and W is the weight matrix. The $\otimes$ operator refers to the Kronecker product, given by the following: if A is an $m \times n$ matrix and B is a $p \times q$ matrix, then the Kronecker product A $\otimes$ B is the $mp \times nq$ block matrix.

After cleaning, epochs corresponding to the frequencies low=[2.50], low-mid= [8.33], mid=[16.67] and high=[33.3] were extracted and averaged for each subject.

Finally, the power spectrum of the epochs was computed using the fast Fourier transform.

E. Joint ICA

The idea of jICA is to establish a link between the modalities by representing the data such that the mutually synchronized information is maximized across the modalities and the information which cannot be mutually represented is removed [25]. Notably, the origin, spatial and temporal structure of the data is essentially irrelevant for jICA, suggesting that data from different subjects, tasks, and modalities can be used jointly for estimation of components given that the sources associated with the modalities are modulate in the same way across all subjects. [25], [28], [29].

Here, we therefore attempt two approaches to joint analysis of SSVEPs. First, we jointly analyze fMRI and time domain EEG. Second, we analyze fMRI and EEG frequency domain data. In our approach, each of the subject's fMRI and EEG data are entered individually into the analysis, and the group of subjects is analyzed into one joint space. We used the jICA algorithm implemented in the Fusion ICA Toolbox (FIT) [30]. Details of the algorithm can be found in [25].

These data are presumably generated by mixing some underlying components of brain activity. Thus, the purpose is to find the original components of brain activity.

Assume a set of latent non-Gaussian neuronal sources as,

$$s = (s_1, s_2, s_3, ..., s_n)^T \tag{2}$$

The responses s are transformed by an unknown mixing matrix A to observe the normally distributed signal X, such that

$$x = As \tag{3}$$

The features and sources of the mixtures are observed in the EEG time (or frequency) signal E at time (or frequency) points t and channel c as $A^E s$

$$x^E = [{x_1}^E(tc), {x_2}^E(tc), ..., {x_n}^E(tc)]^T \tag{4}$$

Similarly, for the fMRI volumes F at respective voxels v we can express as $A^F s$

$$x^F = [{x_1}^F(v), {x_2}^F(v), ..., {x_n}^F(v)]^T \tag{5}$$

The fused signals can then be extracted from the common space as:

$$y^{EF} = [{x_1}^{EF}(tcv), {y_2}^{EF}(tcv), ..., {y_n}^{EF}(tcv)]^T \tag{6}$$

The resulting equation can be expressed as $y = Wx$. The equation to compute the common unmixing matrix W and the fused EEG and fMRI sources, u^{EF}, is then

$$\Delta W = \eta\{I - 2y^{EF}(u^{EF})^T\}W, \tag{7}$$

where η is the learning rate, and the nonlinearity in the neural network is expressed by:

$$y^{EF} = g(u^{EF}), \tag{8}$$

where

$$g(x) = \frac{1}{1 + e^{-x}} \tag{9}$$

The joint ICA model is a generative model, which means that it describes how the observed data are generated by a process of mixing the components s_i. In order to obtain the sources s_i, the equation can be written as:

$$S = Wx \tag{10}$$

where W is the unmixing matrix. Once the mixing matrix A is assumed, the unmixing matrix can be calculated by performing inverse using least square algorithm.

The inverse of non-square matrix cannot be computed by normal inverse of square matrix, so the linear least square solution is used for the purpose:

$$\text{For } x = As \tag{11}$$

$$A^T x = AA^T s, \tag{12}$$

$$s = (AA^T)^{-1}A^T x, \tag{13}$$

where, in Eq. 10,

$$W = (AA^T)^{-1}A^T \tag{14}$$

III. Results

We first describe the results from the unimodal EEG and fMRI analyses, respectively, and then we show the results for the fused analysis.

A. Unimodal analysis: EEG

The analysis of the EEG activity alone showed the typical steady state oscillation responses (Figure 1A and B), confirming previously published studies [20], [21], [31]. The power of the main SSVEP frequency was very small for the mid frequency band (16.7Hz) and almost non-existent for the high frequency band (26.67Hz). Also, the signals were rather noisy, possibly due to the low number of trials and few subjects.

B. Unimodal analysis: fMRI

The group level fMRI analysis revealed significant activations in the visual cortex for the low and low-mid SSVEP frequency bands ($p<0.05$, corrected for multiple comparisons, Figure 2). The foci of these activation was Talairach coordinates [3, -66, 4] and [9, -68, 3] for the low and low-mid bands, respectively. These coordinates are within the standard variation for the location of the primary visual cortex (V1) reported to be located at approximately [9, ’67, 5] [32]. This finding confirms identified SSVEP activations in previously published fMRI studies [20], [21], [31]. No significant activations were found in the mid and high SSVEP frequency bands (Figure 2).

C. Multimodal analysis: Fused fMRI and EEG

The multimodal analysis was performed for each of the four different frequency bands. For each frequency band, three components (corresponding to the number of subjects) were obtained.

In the temporal domain, the interpretation of the results was severely hampered by noise. This analysis is therefore omitted here. Instead, the frequency domain analysis was sucessful, and the results from this analysis are described in more detail.

Visual cortex components: In the low frequency band, only the harmonics of the SSVEP frequency (2.5Hz) were detected (5Hz and up; Figure 3, top panel). In the low-mid and high frequency bands, in contrast, the joint analysis identified the expected SSVEP oscillation frequencies (at 8.33 and 16.67 Hz, respectively; Figure 3). In all bands, these frequencies were localized to similar regions in the brain (Figure 3, indicated by arrows). These regions corresponded to the primary visual cortex, suggesting that the EEG signal (represented in the frequency domain) the fMRI activity likely represent the same neural substrate.

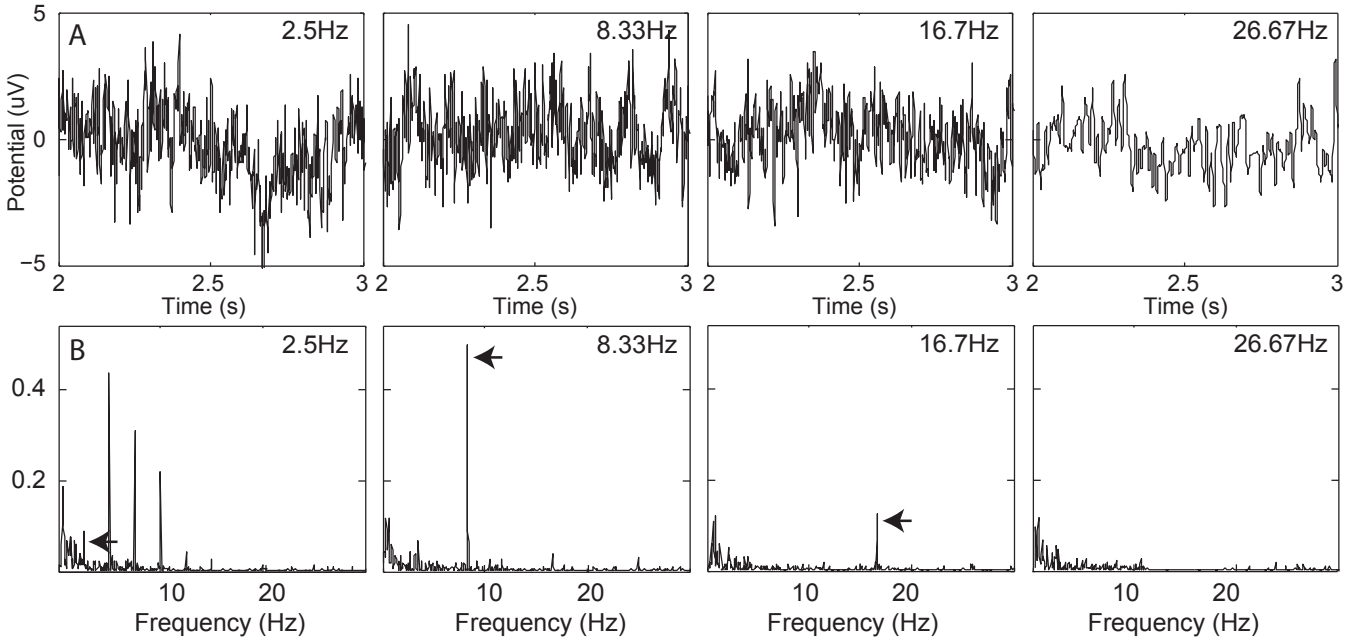

Fig. 1. A) One second snapshot of the EEG signal for different SSVEP frequencies. B) The power of the EEG signal for different SSVEP frequencies.

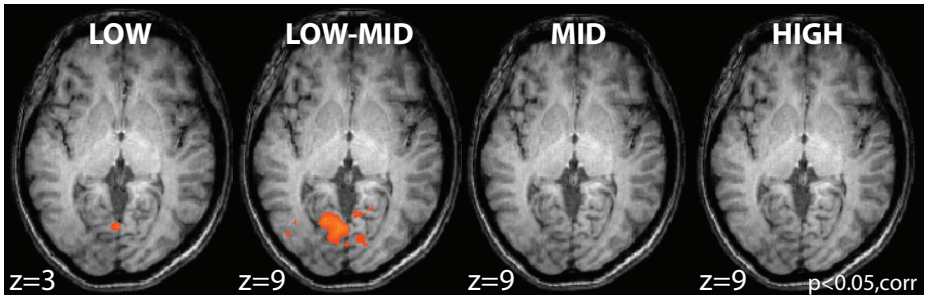

Fig. 2. fMRI contrast maps showing group level brain activations in the primary visual cortex ($p<0.05$, corrected).

Other components: In the high frequency band, no components localized to the visual cortex were found. The other components appeared to reflect mainly noise (Figure 4). This is consistent with the lack of significant activity in this frequency band in the unimodal fMRI analysis and lack of power in the corresponding frequency in the EEG analysis.

IV. Discussion

Our results show that the characteristic temporal feature of SSVEPs – the sustained EEG waveform oscillating with a frequency corresponding to the frequency of the flickering visual stimuli – is localized to the primary visual cortex. Hence, the jICA framework is a feasible approach to fuse separately recorded, frequency domain SSVEP brain responses with fMRI.

The unimodal EEG and fMRI analyses separately confirmed previously published results, including that blocks of flickering stimuli induce a sustained, oscillating wave at the SSVEP frequency and it's harmonics (represented in the EEG) and that the same stimuli activate the primary visual cortex (as shown by fMRI). Going beyond the unimodal analyses, the joint approach revealed a detailed spatiotemporal profile of the neural underpinnings of the signal, providing support for the notion that the temporal characteristics of the EEG at the specific SSVEP frequency is specifically linked to neural activity in the primary visual cortex.

The results obtained from the fusion analysis compares well with studies using simultaneous EEG and fMRI acquisition [21], [31], suggesting that independent recordings of different modalities may be sufficient to study SSVEPs. Independent recordings are appealing since simultaneous EEG-fMRI acquisition is substantially more impractical and the resulting EEG is contaminated by artifacts.

SSVEPs may be recorded in multiple ways, ranging from invasive recordings (e.g. local field potentials and electro-cortiograms), scalp recordings (EEG and magnetoencephalography, MEG), and various optimal imaging techniques (fMRI, near-infrared spectroscopy, NIRS) and other imaging techniques

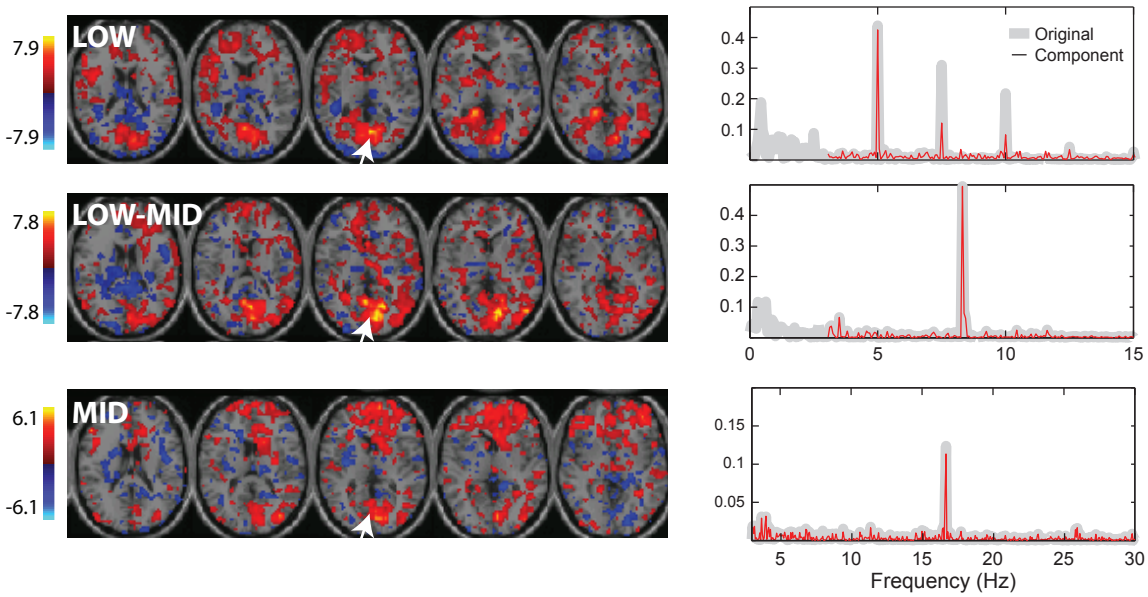

Fig. 3. jICA components that detected the corresponding SSVEP frequencies of each frequency band. The components were all mainly located to the primary visual cortex, indicated by the white arrows.

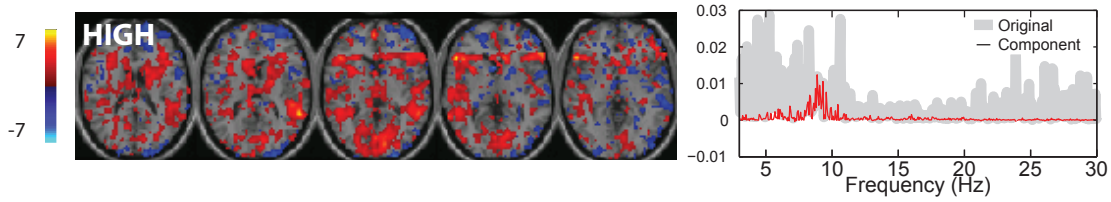

Fig. 4. Example of one component in the high frequency band (26.67-40.0 Hz), showing little else than noise.

(PET, SPECT). Future studies are required to confirm the cross-modal correspondence of the steady-state phenomenon, for example using the proposed jICA framework. Other methods for fusion of EEG and fMRI during SSVEPs are feasible, including canonical correlation analysis (CCA) as well as CCA + ICA.

We found that SSVEP frequencies of over approximately 16.7Hz elicited low brain responses, both in the fMRI and EEG domains, and the resulting fusion was not successful. Also, the multimodal results obtained from the time domain were too noisy to be interpretable. This was likely due to lack of power, primarily due to the very low number of studied subjects. Further studies with larger sample sizes are needed to substantitate this finding.

Having demonstrated the feasibility of the jICA approach for SSVEPs, we have paved the road towards future refined studies with more subjects and more challenging research questions. The proposed method should, for example, be ideal for testing a key question regarding the generative mechanisms behind SSVEPs: whether there is a sequence of sources visible in the results.

ACKNOWLEDGMENT

This work was supported by grants from the Wenner-Gren Foundations (to M.B), and the European Union Seventh Framework Programme (FP7/2007-2013) under grant agreement nr PIOF-GA-2012-302896 (to M.B.).

REFERENCES

[1] F.-B. Vialatte, M. Maurice, J. Dauwels, and A. Cichocki, "Steady-state visually evoked potentials: focus on essential paradigms and future perspectives." *Prog Neurobiol*, vol. 90, no. 4, pp. 418–438, Apr 2010. [Online]. Available: http://dx.doi.org/10.1016/j.pneurobio.2009.11.005

[2] S. T. Morgan, J. C. Hansen, and S. A. Hillyard, "Selective attention to stimulus location modulates the steady-state visual evoked potential." *Proc Natl Acad Sci U S A*, vol. 93, no. 10, pp. 4770–4774, May 1996.

[3] R. Wang, X. Gao, and S. Gao, "A study on binocular rivalry based on the steady state vep." *Conf Proc IEEE Eng Med Biol Soc*, vol. 1, pp. 259–262, 2004. [Online]. Available: http://dx.doi.org/10.1109/IEMBS.2004.1403141

[4] D. Sutoyo and R. Srinivasan, "Nonlinear ssvep responses are sensitive to the perceptual binding of visual hemifields during conventional 'eye' rivalry and interocular 'percept' rivalry." *Brain Res*, vol. 1251, pp. 245–255, Jan 2009. [Online]. Available: http://dx.doi.org/10.1016/j.brainres.2008.09.086

[5] K. A. Ellis, R. B. Silberstein, and P. J. Nathan, "Exploring the temporal dynamics of the spatial working memory n-back task using steady state visual evoked potentials (ssvep)." *Neuroimage*, vol. 31, no. 4, pp. 1741–1751, Jul 2006. [Online]. Available: http://dx.doi.org/10.1016/j.neuroimage.2006.02.014

[6] H. Macpherson, A. Pipingas, and R. Silberstein, "A steady state visually evoked potential investigation of memory and ageing." *Brain Cogn*, vol. 69, no. 3, pp. 571–579, Apr 2009. [Online]. Available: http://dx.doi.org/10.1016/j.bandc.2008.12.003

[7] W. M. Perlstein, M. A. Cole, M. Larson, K. Kelly, P. Seignourel, and A. Keil, "Steady-state visual evoked potentials reveal frontally-mediated working memory activity in humans." *Neurosci Lett*, vol. 342, no. 3, pp. 191–195, May 2003.

[8] R. B. Silberstein, P. L. Nunez, A. Pipingas, P. Harris, and F. Danieli, "Steady state visually evoked potential (ssvep) topography in a graded working memory task." *Int J Psychophysiol*, vol. 42, no. 2, pp. 219–232, Oct 2001.

[9] Z. Wu and D. Yao, "The influence of cognitive tasks on different frequencies steady-state visual evoked potentials." *Brain Topogr*, vol. 20, no. 2, pp. 97–104, 2007. [Online]. Available: http://dx.doi.org/10.1007/s10548-007-0035-0

[10] Z. Wu, D. Yao, Y. Tang, Y. Huang, and S. Su, "Amplitude modulation of steady-state visual evoked potentials by event-related potentials in a working memory task." *J Biol Phys*, vol. 36, no. 3, pp. 261–271, Jun 2010. [Online]. Available: http://dx.doi.org/10.1007/s10867-009-9181-9

[11] D. Neima and D. Regan, "Pattern visual evoked potentials and spatial vision in retrobulbar neuritis and multiple sclerosis." *Arch Neurol*, vol. 41, no. 2, pp. 198–201, Feb 1984.

[12] D. Regan and D. Neima, "Visual fatigue and visual evoked potentials in multiple sclerosis, glaucoma, ocular hypertension and parkinson's disease." *J Neurol Neurosurg Psychiatry*, vol. 47, no. 7, pp. 673–678, Jul 1984.

[13] D. Regan, D. M. Regal, and J. A. Tibbles, "Evoked potentials during recovery from blindness recorded serially from an infant and his normally sighted twin." *Electroencephalogr Clin Neurophysiol*, vol. 54, no. 4, pp. 465–468, Oct 1982.

[14] Z. Yan and X. Gao, "Functional connectivity analysis of steady-state visual evoked potentials." *Neurosci Lett*, vol. 499, no. 3, pp. 199–203, Jul 2011. [Online]. Available: http://dx.doi.org/10.1016/j.neulet.2011.05.061

[15] K. Kaspar, U. Hassler, U. Martens, N. Trujillo-Barreto, and T. Gruber, "Steady-state visually evoked potential correlates of object recognition." *Brain Res*, vol. 1343, pp. 112–121, Jul 2010. [Online]. Available: http://dx.doi.org/10.1016/j.brainres.2010.04.072

[16] B. Z. Allison, C. Brunner, V. Kaiser, G. R. Mller-Putz, C. Neuper, and G. Pfurtscheller, "Toward a hybrid brain-computer interface based on imagined movement and visual attention." *J Neural Eng*, vol. 7, no. 2, p. 26007, Apr 2010. [Online]. Available: http://dx.doi.org/10.1088/1741-2560/7/2/026007

[17] A. Birca, L. Carmant, A. Lortie, P. Vannasing, and M. Lassonde, "Gamma frequency ssvep components differentiate children with febrile seizures from normal controls." *Epilepsia*, vol. 49, no. 11, pp. 1946–1949, Nov 2008. [Online]. Available: http://dx.doi.org/10.1111/j.1528-1167.2008.01878.x

[18] R. H. Hashemi, W. G. Bradley, and C. J. Lisanti, *MRI: the basics*. Lippincott Williams and Wilkins, 2004.

[19] D. G. Norris, "Principles of magnetic resonance assessment of brain function," *Journal of Magnetic Resonance Imaging*, vol. 23, no. 6, pp. 794–807, 2006. [Online]. Available: http://dx.doi.org/10.1002/jmri.20587

[20] A. Bayram, Z. Bayraktaroglu, E. Karahan, B. Erdogan, B. Bilgic, M. Ozker, I. Kasikci, A. D. Duru, A. Ademoglu, C. Oztrk, K. Arikan, N. Tarhan, and T. Demiralp, "Simultaneous eeg/fmri analysis of the resonance phenomena in steady-state visual evoked responses." *Clin EEG Neurosci*, vol. 42, no. 2, pp. 98–106, Apr 2011.

[21] G. Sammer, C. Blecker, H. Gebhardt, P. Kirsch, R. Stark, and D. Vaitl, "Acquisition of typical eeg waveforms during fmri: Ssvep, lrp, and frontal theta." *Neuroimage*, vol. 24, no. 4, pp. 1012–1024, Feb 2005. [Online]. Available: http://dx.doi.org/10.1016/j.neuroimage.2004.10.026

[22] B. J. Fisch, *Fisch & Spehlmann's EEG Primer; Basic Principles of Digital and Analog EEG*, third edition ed. Elsevier Science, 1999.

[23] K. J. Friston, A. P. Holmes, K. J. Worsley, J. P. Poline, C. D. Frith, and R. S. J. Frackowiak, "Statistical parametric maps in functional imaging: A general linear approach," *Human Brain Mapping*, vol. 2, no. 4, pp. 189–210, 1994.

[24] D. Ostwald, C. Porcaro, and A. P. Bagshaw, "An information theoretic approach to eeg-fmri integration of visually evoked responses." *Neuroimage*, vol. 49, no. 1, pp. 498–516, Jan 2010. [Online]. Available: http://dx.doi.org/10.1016/j.neuroimage.2009.07.038

[25] M. Moosmann, T. Eichele, H. Nordby, K. Hugdahl, and V. D. Calhoun, "Joint independent component analysis for simultaneous eeg-fmri: principle and simulation." *Int J Psychophysiol*, vol. 67, no. 3, pp. 212–221, 2008.

[26] J. Mangalathu-Arumana, S. Beardsley, and E. Liebenthal, "Within-subject joint independent component analysis of simultaneous fmri/erp in an auditory oddball paradigm." *Neuroimage*, vol. 60, no. 4, pp. 2247–57, 2012.

[27] C. V., W. L., K. K., E. T., and P. G., "Aberrant processing of deviant stimuli in schizophrenia revealed by fusion of fmri and eeg data." *Acta Neuropsychiatr.*, vol. 22, no. 3, pp. 127–138, 2012.

[28] V. D. Calhoun and T. Adali, "Unmixing fmri with independent component analysis." *IEEE Eng Med Biol Mag*, vol. 25, no. 2, pp. 79–90, 2006.

[29] V. D. Calhoun, T. Adali, G. D. Pearlson, and K. A. Kiehl, "Neuronal chronometry of target detection: fusion of hemodynamic and event-related potential data." *Neuroimage*, vol. 30, no. 2, pp. 544–553, Apr 2006. [Online]. Available: http://dx.doi.org/10.1016/j.neuroimage.2005.08.060

[30] V. C. Srinivas Rachakonda, Jean Liu, "Fusion ica toolbox (fit) manual."

[31] F. Di Russo, S. Pitzalis, T. Aprile, G. Spitoni, F. Patria, A. Stella, D. Spinelli, and S. A. Hillyard, "Spatiotemporal analysis of the cortical sources of the steady-state visual evoked potential." *Hum Brain Mapp*, vol. 28, no. 4, pp. 323–334, Apr 2007. [Online]. Available: http://dx.doi.org/10.1002/hbm.20276

[32] R. F. Dougherty, V. M. Koch, A. A. Brewer, B. Fischer, J. Modersitzki, and B. A. Wandell, "Visual field representations and locations of visual areas v1/2/3 in human visual cortex." *J Vis*, vol. 3, no. 10, pp. 586–598, 2003. [Online]. Available: http://dx.doi.org/10:1167/3.10.1